MECHANICS BASED DESIGN OF STRUCTURES AND MACHINES
Vol. 32, No. 2, pp. 165–193, 2004

Optimal Embedding of Rigid Objects in the Topology Design of Structures

Zhongyan Qian and G. K. Ananthasuresh*

Mechanical Engineering and Applied Mechanics, University of Pennsylvania, Philadelphia, Pennsylvania, USA

ABSTRACT

Extensive published research results exist on the topology design of single-component structures, while multicomponent structural systems have received much less attention. In this article, we present a technique for optimizing the topology of a structure that should be connected to one or more predesigned polygon-shaped components to maximize the stiffness of the overall ensemble. We call it an embedding problem in topology design because predesigned components are to be optimally positioned and oriented within a design region while the connecting structure's topology is optimized simultaneously. Continuous design variables are used to vary the locations of the embedded objects smoothly along with the topology of the connecting structure to apply gradient-based continuous

*Correspondence: G. K. Ananthasuresh, Associate Professor and Graduate Group Chair, Mechanical Engineering and Applied Mechanics, University of Pennsylvania, 220 S. 33rd Street, Philadelphia, PA 19104-6315, USA; Fax: (215) 573-6334; E-mail: gksuresh@seas.upenn.edu.

DOI: 10.1081/SME-120030555 1539-7734 (Print); 1539-7742 (Online)

optimization algorithms. A new material interpolation function on the basis of normal distribution function was used for this purpose. An optimality criteria method combined with the steepest descent method was used to minimize the mean compliance to obtain the stiffest structure for a given volume of material for the connecting structure. As a special case of this method, topology optimization of multicomponent structural systems connected with fasteners was also considered. Illustrative examples are presented.

Key Words: Topology optimization; Multi-component design; Optimal embedding; Optimal placement.

INTRODUCTION

Topology or layout optimization is recognized to be of great importance in the optimal design of structures because choosing a topology is the first step in structural design. The choice of a particular topology will significantly influence subsequent design decisions and eventually the overall performance of the design. Excellent reviews are available on layout optimization (Kirsch, 1989) as well as modern methods of topology optimization (Bendsøe and Sigmund, 2003; Rozvany et al., 1995). The work of Bendsøe and Kikuchi (1988) spurred a lot of interest in topology optimization in the last 15 years. The highlight of this method, called the homogenization-based design method, is the ability to change the topology smoothly with a fixed reference domain. It is essentially a material distribution problem. The original method of Bendsøe and Kikuchi was later simplified and also extended (see Rozvany et al., 1995, for a review). A number of objective criteria including stiffness, strength, natural frequency, flexibility, dynamic response, and stability have been used in the application of this method of structural optimization.

Most of the topology optimization methods developed thus far deal with single-component structures. Usually, as shown in Fig. 1a, the user specifies a design region, boundary conditions, and a fixed volume of a known material. An optimal topology is sought for these specifications. If an object of known stiffness occupies some portion inside the design region or if that region must be occupied by material, it can be accommodated by declaring it as a nondesign region with material at the outset of optimization. The variables associated with nondesign region do not enter the optimization. While this is convenient, it can also be restrictive. For example, some applications may involve one or more objects of known geometry and stiffness to be inside the design region but not necessarily

Marcel Dekker, Inc.
270 Madison Avenue, New York, New York 10016

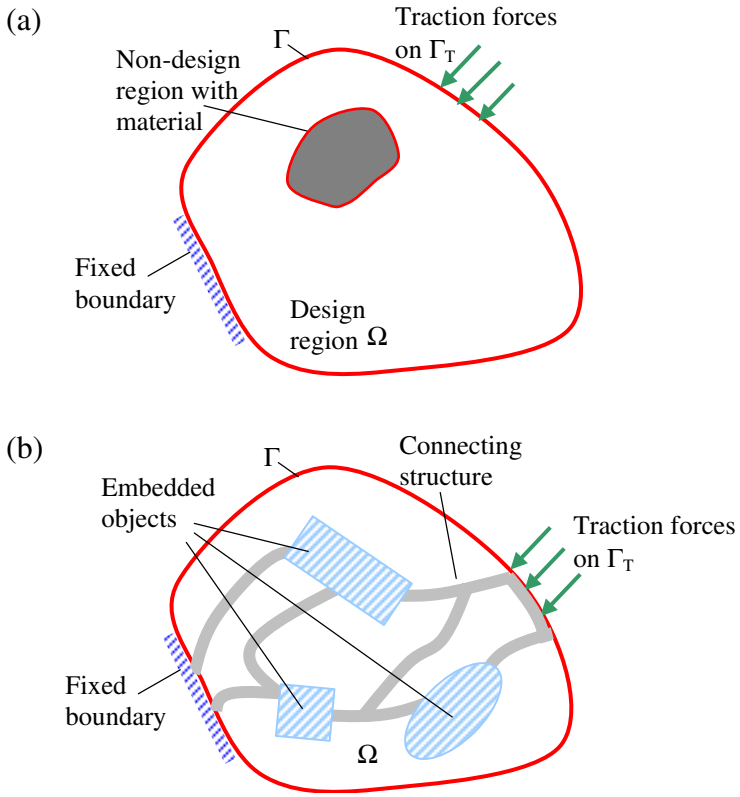

Figure 1. (a) User specifications for the single-component topology optimization with some nondesign region occupied by material and (b) user specifications for topology optimization with embedded objects of known geometry and stiffness but not the location and orientation. *(View this art in color at www.dekker.com.)*

in a fixed location. Such a situation is schematically presented in Fig. 1b. In problems of this type, predesigned components need to be positioned and oriented within the allowable design region, and the structure that connects them is to be designed. It is a problem of optimally embedding predesigned objects into a design region and designing the topology of the connecting structure to optimize a characteristic of the overall assembly. The article focuses on the stiffness aspect of this problem. Some practical implications of this problem and its relationship with multicomponent structural topology optimization are discussed next.

Marcel Dekker, Inc.
270 Madison Avenue, New York, New York 10016

As can be seen in Fig. 1b, the problem considered in this article is concerned with more than one component. Each embedded object is a separate component. The connecting structure too can be thought of as a collection of separate components joined together with the embedded components. The joints are of the rigid type and their physical form may be welded, bolted, riveted, or involve some other type of nonmovable connections. This view of the problem is related to the multicomponent topology problems considered by Johanson et al. (1994), Jiang and Chirehdast (1997), Chickermane and Gea (1997), Yetis and Saitou (2002), and others. In the work of Johanson et al. (1994), a joint location between two or more components was chosen a priori and then the geometry of the components was simultaneously optimized. Jiang and Chirehdast (1997), on the other hand, considered the problem of designing the topology of connections for fixed geometry of components. The two approaches were combined by Chickermane and Gea (1997) by not assuming either the number or the locations of the joints (i.e., the topology of connections) or the geometry of the components. This problem of designing the joint locations along with the topology of the connected components can be viewed as a special case of the problem shown in Fig. 1b. For this, the joints should be viewed as small, embedded objects of known stiffness and geometry. We also address this special case.

The motivation for multicomponent structural assemblies comes from manufacturing and economic considerations. As noted by Lyu and Saitou (2003), it is often more economical to have an assembled system rather than a single-piece structure. But ad hoc decisions about decomposing the system into individual components in the initial stages may hamper the overall performance and cost during the later stages of the design. Therefore, they presented a systematic method to arrive at optimal decomposition strategy in view of manufacturability, assemblability, and a performance criterion such as maximizing stiffness. Similarly, embedding objects arbitrarily is likely to affect the overall optimality. Hence, it is desirable to locate and orient given objects while designing the connecting structure.

The general problem shown in Fig. 1b may also be extended to active structures where the actuators may be thought of as embedded objects. The optimal placement of piezoelectric actuators, as considered by Li et al. (2001), is an example of this type of problem. We do not consider active structures. The scope of this article and its organization are explained as follows.

While many objectives could be considered, we focused only on maximizing the stiffness of the overall system under given loads and volume of material to be used for the connecting structure. We note that the optimal embedding problem of the stiffest structure is nonconvex,

Marcel Dekker, Inc.
270 Madison Avenue, New York, New York 10016

even though the problem of the stiffest structure for a given volume is convex. We examine the origin of this nonconvexity by means of a simple beam example in the next section. This is followed by a description of the general design problem along with a discussion of the objective function, design variables, and constraints. The sensitivity analysis and solution method are described in the following section. After that some numerical examples are presented. Although flexible objects are not precluded by the formulation presented here, only rigid embedded objects with shapes that can be composed using rectangles were considered. A special case where the embedded objects are fixed connections in a multicomponent structure is also presented.

A simple beam example is presented next to clarify the nature of the problem and demonstrate some of its interesting features, such as the origin of nonconvexity.

DESIGN OF A BEAM WITH AN EMBEDDED OBJECT

It is useful to consider a simple example of a beam with an embedded rigid object before the general problem is discussed. Suppose that we intend to design the cross-section of a simply supported beam of length L and volume V^* such that it is the stiffest under a given loading. Assume that a rigid object of length $2l$ is to be embedded within the span of the beam. The location of the rigid object along the axis of the beam is not known, and it should be determined in conjunction with beam's cross-section profile to maximize the stiffness. A lower bound of A_0 on the area of cross-section at any point along the beam's axis is also imposed. The symbols and all the numerical data are shown in Fig. 2 and Table 1.

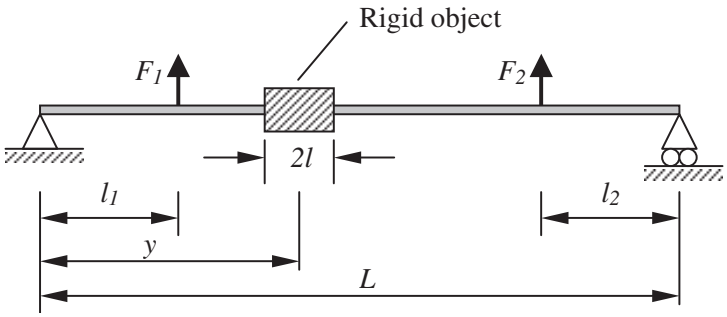

Figure 2. Problem specifications for the beam example.

Table 1. Numerical data for the beam shown in Fig. 1.

$L = 0.27\,\text{m}$	$l = 0.01\,\text{m},\ l_1 = 0.08\,\text{m},\ l_2 = 0.06\,\text{m}$
$h = 0.005\,\text{m}$	$A_0 = 15\,E-6\,\text{m}^2,\ V^* = 13.5\,E-6\,\text{m}^3$
$F_1 = 10\,\text{N},\ F_2 = -20\,\text{N}$	$E = 210\,\text{GPa}$

The objective of maximum stiffness is achieved by minimizing the strain energy stored in the beam. The design variable is $A(x)$, which is the cross-section area along the longitudinal axis of the beam. By assuming rectangular cross-section of constant depth h, the moment of inertia of the cross-section can be written as

$$I(x) = (h^2/12)A(x) = \alpha A(x) \tag{1}$$

Since it is a statically determinate problem, the bending moment in the beam does not depend on the area of cross-section. Therefore, the optimization problem statement can be written as follows. Note that Ω_A represents the span of the beam excluding the portion occupied by the embedded object. That is, $\Omega_A = [0, y-l] \cup [y+l, L]$.

Minimize strain energy

$$\begin{aligned} &= f = \int_{\Omega_A} \frac{M^2(x)}{2E\alpha A(x)}\,dx \\ &= \int_0^{y-l} \frac{M^2(x)}{2E\alpha A(x)}\,dx + \int_{y+l}^{L} \frac{M^2(x)}{2E\alpha A(x)}\,dx \\ &= \int_0^{L} \frac{M^2(x)}{2E\alpha A(x)}\,dx - \int_{y-l}^{y+l} \frac{M^2(x)}{2E\alpha A(x)}\,dx \end{aligned}$$

with respect to $A(x)$ and y, subject to

$$\begin{aligned} &\int_{\Omega_A} A(x)\,dx - V^* \le 0 \\ &A_0 - A(x) \le 0 \end{aligned} \tag{2}$$

where the objective function reflects the fact that the embedded rigid body does not store any strain energy. The Lagrangian L, of the above problem can be written as

Marcel Dekker, Inc.
270 Madison Avenue, New York, New York 10016

$$L = \int_{\Omega_A} \frac{M^2(x)}{2E\alpha A(x)}\, dx + \Lambda\left(\int_{\Omega_A} A(x)\, dx - V_0\right) + \int_{\Omega_A} \lambda(x)(A_0 - A(x))\, dx \tag{3}$$

It should be noted that the Lagrange multiplier Λ, is just an unknown constant while the other Lagrange multiplier $\lambda(x)$ is an unknown function of x due to the global and local nature of the respective constraints. By equating the first variation of L with respect to the design variables $A(x)$ and y to zero, and by using Karush–Kuhn–Tucker conditions for the constrained minimization, we get:

$$\delta_A L = -\frac{M^2(x)}{2\alpha E\, A^2(x)} + \Lambda - \lambda(x) = 0 \quad \forall x \in \Omega_A \tag{4a}$$

$$\delta_y L = -\frac{M^2(y+l)}{2\alpha E\, A(y+l)} + \frac{M^2(y-l)}{2\alpha E\, A(y-l)} = 0 \tag{4b}$$

$$\int_{\Omega_A} A\, dx - V^* \le 0, \quad \Lambda\left\{\int_{\Omega_A} A\, dx - V^*\right\} = 0 \ \text{ and } \ \Lambda \ge 0 \tag{4c}$$

$$A_0 - A(x) \le 0, \quad \lambda(x)\{A_0 - A(x)\} = 0 \ \text{ and } \ \lambda(x) \ge 0\, \forall x \in \Omega_A \tag{4d}$$

Since more material helps decrease the strain energy, the volume constraint will be active. That is, $\Lambda > 0$. From the complementarity condition in Eq. (4d), we see that $\lambda(x)$ is positive only for those values of x at which $A(x) = A_0$. Thus, Ω_A can be divided into two regions: one in which $A(x) = A_0$, $\lambda(x) > 0$ and the other in which $A(x) > A_0$, $\lambda(x) = 0$. The area of cross-section in the latter region can be computed using Eq. (4a). Thus,

$$A(x) = A_0$$

for

$$\lambda(x) = \left(\Lambda - \frac{M^2(x)}{2\alpha E A_0^2}\right) > 0 \tag{5a}$$

$$A(x) = \sqrt{\frac{1}{2\alpha E \Lambda}}|M|$$

for

$$A(x) > A_0, \quad \lambda(x) = 0 \tag{5b}$$

Marcel Dekker, Inc.
270 Madison Avenue, New York, New York 10016

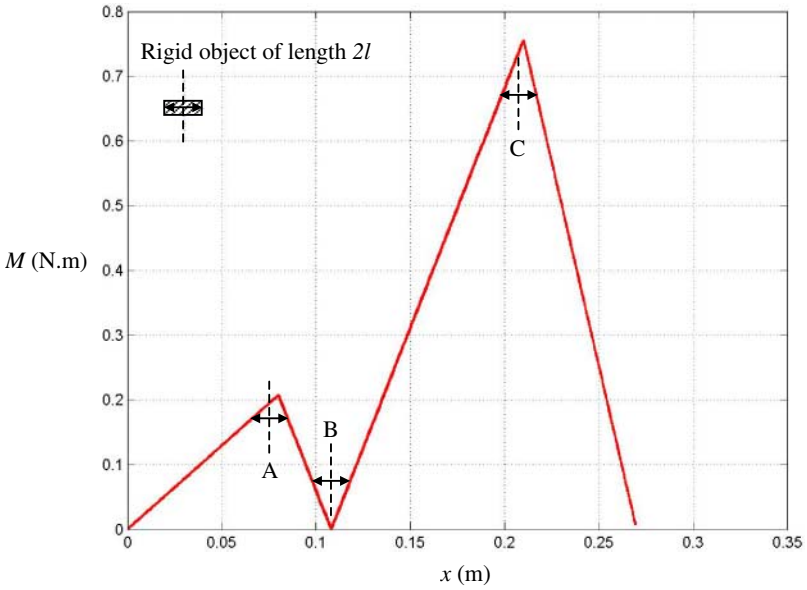

Figure 3. Absolute value of the bending moment of the statically determinate beam of Fig. 2. *(View this art in color at www.dekker.com.)*

which shows that the cross-section area is proportional to the absolute value of the bending moment. From Eqs. (4b), (5a), and (5b), it can be concluded that

$$|M(y-l)| = |M(y+l)| \tag{6}$$

The above equation implies that the absolute values of the bending moments at a distance of l on either side of y are equal at the optimum. In Fig. 3, in which $|M(x)|$ is plotted, we see that there are three points, A, B, and C, that satisfy Eq. (6). The condition in Eq. (6) can also be understood intuitively as explained as follows.

In Eq. (2), the objective function is written in three alternate forms. The last of these shows that the minimum value of the function can be achieved if y is chosen so that the second term is as large as possible. That is, optimum y should correspond to the location where $|M(x)|$ has a local maximum. Referring to Fig. 3, this happens at points A and C. Intuitively, it means that the rigid object should be placed in the region that contributes a large amount to the strain energy. Naturally, this happens

Marcel Dekker, Inc.
270 Madison Avenue, New York, New York 10016

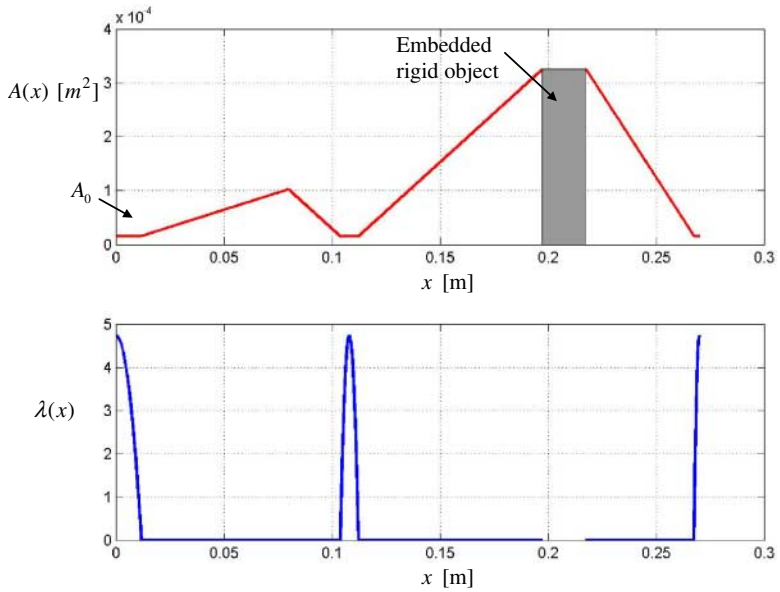

Figure 4. Global minimum solution to the beam problem (a) area of cross-section and the rigid object embedded at the optimum location and (b) $\lambda(x)$ corresponding to the global minimum solution. *(View this art in color at www.dekker.com.)*

at the regions of local maxima of $|M(x)|$ since the strain energy is proportional to $|M(x)|$. Likewise, a local maximum of the objective function occurs when $|M(x)|$ has a local minimum and the rigid object of length $2l$ could be placed there. This happens at point B. Thus, this example shows that the problem of maximizing stiffness becomes nonconvex in the presence of an optimally embedded rigid object. This phenomenon will be noticed in the more general problems solved later in this article.

Although finding the global minimum in a general problem is not easy, this problem can be solved for the global minimum since it is clear from Fig. 3 that point C corresponds to the optimum y, which is equal to 0.2074 m. Using this value, Eqs. (4) and (5) can be iteratively solved to find the values of Λ, $A(x)$, and $\lambda(x)$. Iteration is necessary because apportioning Ω_A into regions where $A(x) = A_0$ or $A(x) > A_0$ cannot be decided in one step. The solution is shown in Fig. 4. The plot at the top shows the optimum area of cross-section and the bottom plot $\lambda(x)$. The corresponding value of Λ is 4.7283. The cross-section area plot

shows the rigid object embedded at the optimum location as determined by $y = 0.2074\,\text{m}$.

Next, we consider the general problem of topology optimization with embedded objects. The insight gained from the simple beam example of this section helps understand the nonconvexity and other characteristics of the solutions to the general problem.

PROBLEM FORMULATION

The schematic of the general problem was shown in Fig. 1b. The inputs to this design problem are a design region Ω of arbitrary shape, applied traction forces $\mathbf{f}$ on the boundary Γ of Ω, fixed boundary condition on some portion of Γ, and m objects of known geometry and material. The objective is to position and to orient given m objects and connect them to the applied tractions and fixed boundary using a connecting structure to maximize the stiffness of the overall assembly. The connection between the connecting structure and the embedded objects is assumed to be rigid, such as in a welded joint. As is common in the optimal design of stiff structures, the *mean compliance* is used as the measure of stiffness. Mean compliance J is given by

$$J(\mathbf{u}) = \int_{\Gamma_T} \mathbf{f} \cdot \mathbf{u}\, d\Gamma \tag{7}$$

where $\mathbf{u}$ denotes the displacements at the static equilibrium of the structure under applied traction loads. At equilibrium, the mean compliance is equal to twice the strain energy stored in the structure and, therefore, the smaller the mean compliance the stiffer the structure. Thus, the function in Eq. (7) is to be minimized. The maximum permissible volume V^* of the connecting structure is specified in the problem and it is posed as an inequality constraint, as shown below.

$$\int_{\Omega} d\Omega - V^* \leq 0 \tag{8}$$

Defining the design variables to smoothly vary the positions and orientations of the embedded objects as well as the topology of the connecting structure on a fixed reference domain is necessary to apply gradient-based optimization algorithms to solve this problem. Identification of such design variables, referred to as *design parameterization*, is described next.

MARCEL DEKKER, INC.
270 Madison Avenue, New York, New York 10016

Design Parameterization for the Connecting Structure

As is well known, topology optimization is a problem of distributing less material than what can fit into in a given design region. If we assign a design variable for every point in the region then that variable assumes "0 or 1" binary parameterization with "0" implying material being there and "1" implying a void. Large-scale optimization problems involving binary variables are difficult to solve with deterministic algorithms, which prompted continuous parameterization in various forms. The microstructure of a composite material made up of material and void used in the homogenization-based design method by Bendsøe and Kikuchi (1988) or in a slightly different form by Chickermane and Gea (1997), a power law model used in simple isotropic material with penalty (SIMP) (Rozvany et al., 1989), a peak function material interpolation model by Yin and Ananthasuresh (2001), topological functions by De Reuiter and van Keulen (2000), and level-set based methods by Wang et al. (2003) are some of the many possible ways of continuous design parameterization. In SIMP parameterization, a fictitious density ρ defined at every point is used to vary the relevant material properties (e.g., E) as shown below.

$$E = \rho^{\eta} E_0 \quad 0 \leq \rho \leq 1 \tag{9}$$

where E is the interpolated Young's modulus, E_0 is the Young's modulus of the material, and η is a penalty parameter, usually chosen to be larger than three. In the peak function parameterization, ρ is simply a continuous variable defined for every point and is used in a normal distribution function to interpolate a material property as shown below.

$$E = \exp\left(-\frac{(\rho-\mu)^2}{\sigma^2}\right) E_0 \quad -\infty \leq \rho \leq \infty \tag{10}$$

When the "standard deviation" σ is very small, material exists at a point only when ρ at that point is equal to μ. For any other value of ρ, the material is absent at the point. When σ is not small, some "intermediate" material would exist even for values of ρ that are close to μ. Beginning with a moderately large value of σ and then gradually making it smaller in every iteration leads to proper "0 or 1" type material distribution within the design region at the end of the iterative process. This technique has the advantage of not restricting ρ between upper and lower limits and has allows for the ability to distribute multiple materials [see Eq. (11)] without increasing the number of design variables at a point (Yin and Ananthasuresh, 2001).

Marcel Dekker, Inc.
270 Madison Avenue, New York, New York 10016

$$E = \sum_{i=1}^{m} \exp\left(-\frac{(\rho - \mu_i)^2}{\sigma_i^2}\right) E_i \tag{11}$$

where m is the number of materials, and μ_i and σ_i are specified appropriately.

We use this parameterization for the connecting structure in this article but only with a single material. Thus, the connecting structure needs $\rho(\mathbf{x})$ as the design variable at every point with coordinates $\mathbf{x}$ in the design region Ω. In a discretized finite element model, there will be a ρ associated with each element.

Design Parameterization for the Embedded Objects

As stated earlier, the geometry and the material properties of the embedded objects are assumed to be known. So, the design variables associated with each of them are simply the location of the centroid (or any other convenient point) and an orientation. In three-dimensions, each object will have six design variables and only three in two dimensions. Since the examples considered in this article are only in two dimensions, the schematic in Fig. 5 shows these variables, i.e., (x_i, y_i) for translations, and ϕ_i for orientation with $i = 1, 2$ for two objects.

Within the object i, the Young's modulus will be equal to the given value of Young's modulus E_i of that object. If the object is assumed to be rigid, this value will be very large. Now, consider a point outside an object

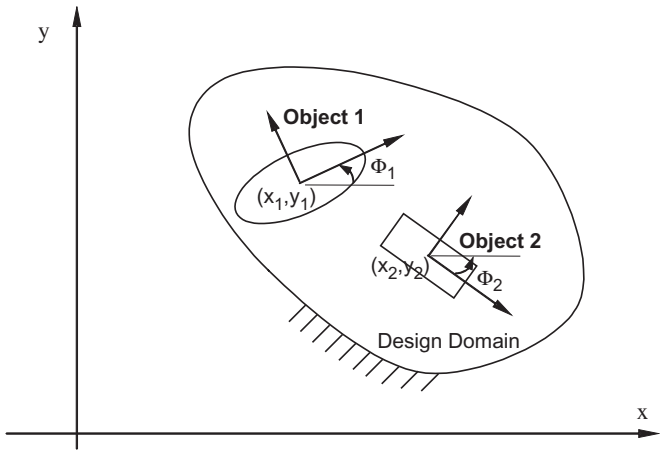

Figure 5. Design variables for optimal embedding of objects of known shape and material.

but very close to the boundary. Suppose that when this object moves, this point lies inside the object. For this situation, the Young's modulus of the point jumps to a different value, creating a discontinuity. To resolve this situation, we model the transition smoothly using the normal distribution function in Eq. (10) in a different way as follows. Although this concept is general and is applicable to the three dimensional case, from this point onward, we will write it only for two dimensions.

In the parameterization scheme adopted, the Young's modulus at every point is interpolated for both the connecting structure and the embedded objects, as shown below.

$$E(x, y) = \hat{E}_0 + \sum_{i=1}^{n} \hat{E}_i \tag{12}$$

where

$$\begin{aligned} \hat{E}_0 &= E_0 \exp\left(-\frac{(\rho - \mu)^2}{\sigma^2}\right) \\ \hat{E}_i &= E_i \exp\left(-\frac{(\Delta\tilde{x}_i)^\eta}{\sigma_{xi}^2} - \frac{(\Delta\tilde{y}_i)^\eta}{\sigma_{yi}^2}\right) \\ \begin{Bmatrix} \Delta\tilde{x}_i \\ \Delta\tilde{y}_i \end{Bmatrix} &= \begin{bmatrix} \cos\phi_i & \sin\phi_i \\ -\sin\phi_i & \cos\phi_i \end{bmatrix} \begin{Bmatrix} x - x_i \\ y - y_i \end{Bmatrix} \end{aligned} \tag{13}$$

As shown in the second equation of Eq. (13), we can model rectangular objects when we choose the exponent η to be larger than or equal to 4. By combining several rectangular objects of various sizes, several other shapes can also be obtained. The combination of several rectangles is not shown in Eq. (13) but can easily be imagined by the readers. Graphical portrayal of Eq. (13) for a square object and a nonconvex object is shown in Fig. 6a. In this case, E_0 is assumed to be uniform in all of Ω except the area occupied by the objects. Rectangle's length and width are controlled by σ_{xi} and σ_{yi}, which are specified based on the object to be embedded. The transition between object's material property (in this case, the Young's modulus) and the vicinity is controlled by the exponent η: the larger the value of η, the sharper the transition. The contours of the surface of Fig. 6a are shown in Fig. 6b. Here, $\eta = 4$, and gradual transition can be seen. It should be noted that however large η is, the continuity is ensured in this material interpolation. In practice, η, in fact, can be chosen to reflect the stiffness of the type of connection (bolted, riveted, welded, etc.) at the interface between the object and the connecting structure.

Marcel Dekker, Inc.
270 Madison Avenue, New York, New York 10016

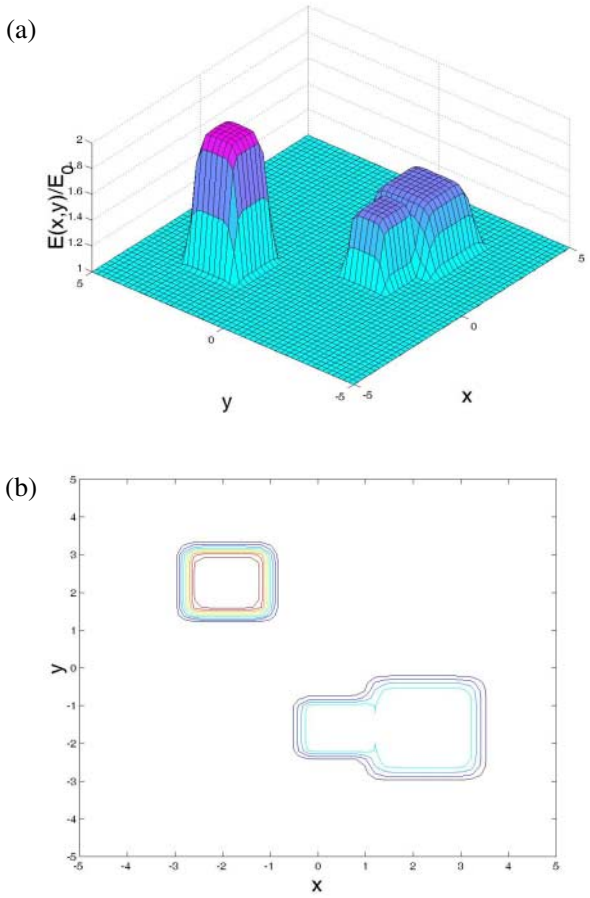

Figure 6. (a) Material interpolation for a square object and a nonconvex object embedded into the design region and (b) the corresponding contour plot.

Design Parameterization for Multicomponent Topology Optimization Problem

In the work of Chickermane and Gea (1997), simultaneous topology optimization of multiple, connected components was presented. There, in addition to the design variables corresponding to the material distribution in each component, additional variables were defined to vary the "densities" of rigid connections between the two in a predefined overlapping region.

Each rigid connection was assigned a continuous variable with tuning that eventually makes the connection "0" or "1" to decide whether it remains at the end (value of "1") or not (value of "0"). This problem can be posed as a special case of the embedding problem if we treat the rigid connections as embedded objects between two or more components. If there are m connections to be located, continuous design variables c_i can be used to model the stiffness k_i^s of the connections as follows.

$$k_i^s = k_0^s \exp\left(-\frac{(c_i - \mu_i)^2}{\sigma_i^2}\right) \quad \text{for} \quad i = 1, 2, \ldots, m \tag{14}$$

where k_0^s is the stiffness of the connection when it is "fully" present. With a constraint on the total number of connections, their number can be controlled.

Optimization Problem Statement

Using the above objective function, constraint, and design variables, the optimization problem can now be stated as follows.

$$\text{Minimize } J(\mathbf{u}) = \int_{\Gamma_T} \mathbf{f} \cdot \mathbf{u}\, d\tilde{A} \tag{15a}$$

with respect to: $\mathbf{b} = \{\rho(x, y), (x, y, \phi)_i\}, i = 1, 2, \ldots, m$

Subject to:

$$\nabla \cdot (\mathbf{D}(\mathbf{b})\, \boldsymbol{\varepsilon}(\mathbf{u})) + \mathbf{f}_b = 0 \quad \forall x \in \Omega \text{ and boundary conditions.} \tag{15b}$$

$$\int_\Omega \exp\left(-\frac{(\rho - \mu)^2}{\sigma^2}\right) d\Omega - V^* \leq 0 \tag{15c}$$

$$\begin{aligned} x_i^l \leq x_i \leq x_i^u \\ y_i^l \leq y_i \leq y_i^u \end{aligned} \qquad i = 1, 2, \ldots, m \tag{15d}$$

and constraints to avoid intersections among the objects.

The equation of static equilibrium is expressed in Eq. (15b). Here, $\mathbf{D}(\mathbf{b})$ is the matrix of material properties (i.e., Young's modulus and Poisson's ratio for an isotropic material) relating stress and strain vectors. It depends on the design variables ($\mathbf{b}$), as shown in Eq. (12). And, $\boldsymbol{\varepsilon}$ is the linear strain in the vector form given by given by $\{\partial u_x/\partial x, \partial u_y/\partial y, \partial u_z/\partial z, \partial u_x/\partial y + \partial u_y/\partial x, \partial u_y/\partial z + \partial u_z/\partial y, \partial u_z/\partial x + \partial u_x/\partial z\}^T$. The body force $\mathbf{f}_b$ is assumed to be absent in the problems considered in this work. The boundary conditions include imposed conditions on the displacements

Marcel Dekker, Inc.
270 Madison Avenue, New York, New York 10016

and traction forces. The volume constraint is given by Eq. (15c). The inequality constraints in Eq. (15d) specify the upper and lower bounds on the coordinates of the centroids (or other convenient points of reference) of the objects. In general, the bounds can be the bounds of Ω unless there is some other reason for a particular object. The last constraint, to avoid intersections among objects, can be implemented as follows since we know the shapes and sizes of the objects. Consider two objects j and k for which the diameters of the circles that enclose them completely are d_j and d_k, respectively. The constraint to avoid intersection between them can be posed as follows.

$$(x_j - x_k)^2 + (y_j - y_k)^2 - (d_j + d_k)^2 \geq 0 \tag{16}$$

If there are three objects, three such constraints are necessary, and so on. These constraints are also continuous and differentiable and thus do not come in the way of the application of continuous optimization algorithms. If the objects are slender, a different form of the constraints that avoids the intersection of elongated ellipses will be necessary.

SOLUTION METHOD

Unlike the simple beam problem described in an earlier section, the general problem of the previous section cannot be solved analytically. Hence, it is necessary to use a numerical optimization algorithm as opposed to analytical manipulation of the necessary conditions for a constrained minimum. The necessary conditions can be written for the continuous representation of the problem as shown in Eq. (15). However, it is more instructive to use the discretized finite element representation from the viewpoint of implementation of the solution procedure. The discretized version of Eq. (15) in a plane using the plane-stress elements can be written as follows.

$$\text{Minimize } J(\mathbf{U}) = \mathbf{F}^T\mathbf{U} \tag{16a}$$

$$\text{With respect to: } \mathbf{b} = \{\rho_j, (x, y, \phi)_i\}, \quad i = 1, 2, \ldots, m; \; j = 1, 2, \ldots, N$$

Subject to:

$$\mathbf{KU} = \mathbf{f} \text{ and displacement boundary conditions.} \tag{16b}$$

$$\sum_{i=1}^{N} (tA_i\rho_i) - V^* = V - V^* \leq 0 \tag{16c}$$

$$\begin{matrix} x_i^l \leq x_i \leq x_i^u \\ y_i^l \leq y_i \leq y_i^u \end{matrix} \quad i = 1, 2, \ldots, m \tag{16d}$$

and constraints to avoid intersections among the objects.

MARCEL DEKKER, INC.
270 Madison Avenue, New York, New York 10016

where Eqs. (16a) through (16d) correspond to Eqs. (15a) through (15d) and the new symbols represent the following quantities:

$\mathbf{U}$ = vector describing the nodal degrees of freedom of all the plane-stress elements
$\mathbf{F}$ = vector of external forces applied at all nodal degrees of freedom
$\mathbf{K}$ = global stiffness matrix of the entire structure
N = number of plane-stress elements
A_i = area of element i
t = thickness of the two-dimensional domain assumed to be uniform everywhere

The global stiffness matrix $\mathbf{K}$ is assembled from element stiffness matrices k_i^e, $i = 1, 2, \ldots N$, given by

$$\mathbf{k}_i^e = \int_{A_e} \mathbf{B}^{\mathrm{T}} \mathbf{D}(\mathbf{b}) \mathbf{B}\, dA \tag{17}$$

where, $\mathbf{B}$ is the strain-displacement matrix and involves shape functions but not the design variables, and $\mathbf{D}(\mathbf{b})$ is constitutive stress-strain matrix and involves only material properties (Young's modulus and Poisson's ratio) interpolated using the design variables as per Eq. (12).

Since we used a gradient-based optimization algorithm to solve the above problem, we need to perform analytical sensitivity analysis for computational efficiency in computing the gradients with respect to the design variables: $\rho_i (i = 1, 2, \ldots N)$ for the N plane-stress elements, and $3m$ variables for m embedded objects.

Sensitivity Analysis

The gradient of the displacement vector $\mathbf{U}$ with respect to the design variables is the primary focus in the sensitivity analysis as the gradients of the remaining quantities can easily be computed using the gradient of $\mathbf{U}$ or without it (e.g., the gradient of the volume constraint). Since the loads are independent of the design variables, by using Eq. (16b), the gradient of $\mathbf{U}$ can be obtained as follows.

$$\mathbf{K} \frac{\partial \mathbf{U}}{\partial b_i} = -\frac{\partial K}{\partial b_i} \mathbf{U} \quad i = 1, 2, \ldots (N + 3m) \tag{18}$$

Since the number of variables exceeds the number of constraints, adjoint method (Haftka and Gurdal, 1989) is more efficient than solving Eq. (18) for each variable. In computing $\partial \mathbf{K} / \partial b_i$, we need the partial

Marcel Dekker, Inc.
270 Madison Avenue, New York, New York 10016

derivatives of E (Young's modulus) with respect to each design variable. These are shown as:

$$\frac{\partial E}{\partial \tilde{n}_k} = -2E_0 \frac{\tilde{n}_k - \mu}{\sigma^2} \exp\left(-\frac{(\tilde{n}_k - \mu)^2}{\sigma^2}\right) \qquad k = 1, 2, \ldots N \tag{19a}$$

$$\frac{\partial E}{\partial x_i} = -\hat{E}_i \eta \left(\frac{(\Delta\tilde{x}_i)^{\eta-1}}{2\sigma_{xi}^2}\frac{\partial \Delta\tilde{x}_i}{\partial x_i} + \frac{(\Delta\tilde{y}_i)^{\eta-1}}{2\sigma_{yi}^2}\frac{\partial \Delta\tilde{y}_i}{\partial x_i}\right) \qquad i = 1, 2, \ldots m \tag{19b}$$

$$\frac{\partial E}{\partial y_i} = -\hat{E}_i \eta \left(\frac{(\Delta\tilde{x}_i)^{\eta-1}}{2\sigma_{xi}^2}\frac{\partial \Delta\tilde{x}_i}{\partial y_i} + \frac{(\Delta\tilde{y}_i)^{\eta-1}}{2\sigma_{yi}^2}\frac{\partial \Delta\tilde{y}_i}{\partial y_i}\right) \qquad i = 1, 2, \ldots m \tag{19c}$$

$$\frac{\partial E}{\partial \phi_i} = -\hat{E}_i \eta \left(\frac{(\Delta\tilde{x}_i)^{\eta-1}}{2\sigma_{xi}^2}\frac{\partial \Delta\tilde{x}_i}{\partial \phi_i} + \frac{(\Delta\tilde{y}_i)^{\eta-1}}{2\sigma_{yi}^2}\frac{\partial \Delta\tilde{y}_i}{\partial \phi_i}\right) \qquad i = 1, 2, \ldots m \tag{19d}$$

Computing the gradients of the volume constraint [Eq. (16c)] and the inter-object intersection constraints is straightforward.

Variable Update Scheme

Topology optimization problems can be solved using many different techniques, such as the optimality criteria methods (OC), sequential quadratic programming (SQP), sequential linear programming (SLP), method of moving asymptotes (MMA), and others. We used an OC-type method along the lines of Yin and Yang (2001) and augmented it with a steepest descent method.

By writing the Lagrangian of the optimization problem in Eq. (16) and equating its gradient with respect to the design variables to zero, an optimality criterion can be derived as explained below:

$$\frac{\partial J}{\partial b_j} + \Lambda \frac{\partial V}{\partial b_j} = 0 \quad j = 1, 2, \ldots (N + 3m) \tag{20}$$

Using the above criterion for N ρ-variables and m ϕ-variables, an iterative update formula for these design variables is set up as:

$$b_j^{\text{new}} = \begin{cases} \max(b_j^{\min}, b_j^{\text{old}} - \text{move}) & \text{if} \quad P_j \le \max(b_j^{\min}, b_j^{\text{old}} - \text{move}) \\ P_j \quad \text{if} \quad \max(b_j^{\min}, b_j^{\text{old}} - \text{move}) < P < \min(b_j^{\min}, b_j^{\text{old}} + \text{move}), & \\ \quad j = 1, 2, \ldots, N + m & \\ \min(b_j^{\min}, b_j^{\text{old}} + \text{move}) & \text{if} \quad \min(b_{\max}, b_j^{\text{old}} + \text{move}) \le P_j \end{cases} \tag{21}$$

where move $= (1+\delta)b_j^{\text{old}}$ with δ as a relative move limit, and P_j a quantity that can be derived from Eq. (20) in one of two ways. In the first, the design variable is updated by multiplying by a quantity that eventually should converge to unity. In the other, a quantity that eventually should converge to zero is added to the design variable. It is usual in these methods to use some parameters that control how much change is permitted in the design variables at a given iteration. These parameters are obtained with the experience gained from numerical experiments with a given class of problems. The two methods are:

$$P_j = b_j^{\text{old}}\left(-\frac{\partial J/\partial b_j}{\lambda(\partial V/\partial b_j)}\right)^{\alpha} \tag{22a}$$

$$P_j = \beta b_j^{\text{old}} - (1-\beta)b_j^{\text{old}}\left(-\frac{\partial J/\partial b_j}{\lambda(\partial V/\partial b_j)}\right) \tag{22b}$$

where α and β are numerical damping coefficients. The Lagrange multiplier Λ is obtained in an inner loop in every iteration step. To update the Lagrangian multiplier Λ, the modified Newton–Raphson iteration scheme is utilized to solve the nonlinear constraint equation (Yin and Yang, 2001).

For the remaining $2m$ design variables, which determine the position of flexible objects, we use the steepest descent method. This is because, unlike the other variables that can take any value in the range $(-\infty, \infty)$, these are bounded by the constraints in Eq. (16c). The optimality criterion-based update scheme, if used, would need additional Lagrange multipliers that also need to be updated in every iteration. To circumvent this, a steepest descent algorithm is used for these variables. Thus, the two translation variables of each embedded object are updated as follows:

$$x_i^{\text{new}} = x_i + \alpha S_i \quad \text{for} \quad i = 1, 2, \ldots 2m \tag{23a}$$

$$y_i^{\text{new}} = y_i + \alpha S_i \quad \text{for} \quad i = 1, 2, \ldots 2m \tag{23b}$$

$$S_i = \frac{-\partial J/\partial x_i}{\sqrt{(\partial J/\partial x_i)^2 + (\partial J/\partial y_i)^2}} \quad \text{for} \quad i = 1, 2, \ldots 2m \tag{23c}$$

where $\mathbf{S}$ is the unit vector of size $2m \times 1$ representing the steepest descent direction and α is the step length for an iteration. The value of α is determined using a line-search algorithm. Thus, we combined the optimality criteria method with a steepest descent method to solve this problem. Other methods mentioned earlier can also be used but this modified optimality criteria method gave satisfactory results to illustrate

Marcel Dekker, Inc.
270 Madison Avenue, New York, New York 10016

the validity of the new formulation and the concept of topology optimization with embedded objects. Some numerical examples follow.

NUMERICAL EXAMPLES AND DISCUSSION

The solution algorithm was implemented in MATLAB (2003) technical programming language. All structures were modeled using eight-noded quadrilateral plane-stress elements. In addition to the examples of single and multiple embedded objects, the examples of multicomponent structures with rigid connections are also included in this section.

Embedding a Single Rigid Object

The specifications for the first example problem are shown in Fig. 7a. The design region is meshed into 48×38 eight-noded quadrilateral plane-stress elements. The volume constraint was set at 50% of the total design region, and parameters controlling the interpolation of the material properties were set at $\mu = 1.0$ and $\sigma = 0.1$. The Young's modulus of the embedded rectangular object is assumed to be large to simulate the effect of a rigid body. In this case, it is 10 times that of the material of the connecting structure. A load is applied at the lower left corner while the right edge is fixed. The orientation of the object for the initial guess is as shown in Fig. 7b. The optimal solution is shown in Fig. 7c. As seen in the figure, the rigid object, together with the connecting structure, resembles the widely reported single component optimal structure under this loading and boundary conditions.

The embedding of the object into a structure raises some intuitive questions that can be explained using this and other examples. Intuitively, the result of Fig. 7c might surprise some investigators who think that the rigid object should get embedded at the fixed surface in the optimal solution. It is generally correct to think that way because it is equivalent to extending the fixed surface into the design region and because the stress is usually high at the fixed surface(s). But it did not happen in the solution shown in Fig. 7c. This can be explained in light of the analytical insight gained from the beam problem presented earlier. Recall that the embedded object is placed at the location where the absolute value of the maximum stress. Consider the von Mises stress distribution (Fig. 8) of the optimal solution obtained when no embedded objects are considered. Notice that the highest stress occurs, as expected,

Marcel Dekker, Inc.
270 Madison Avenue, New York, New York 10016

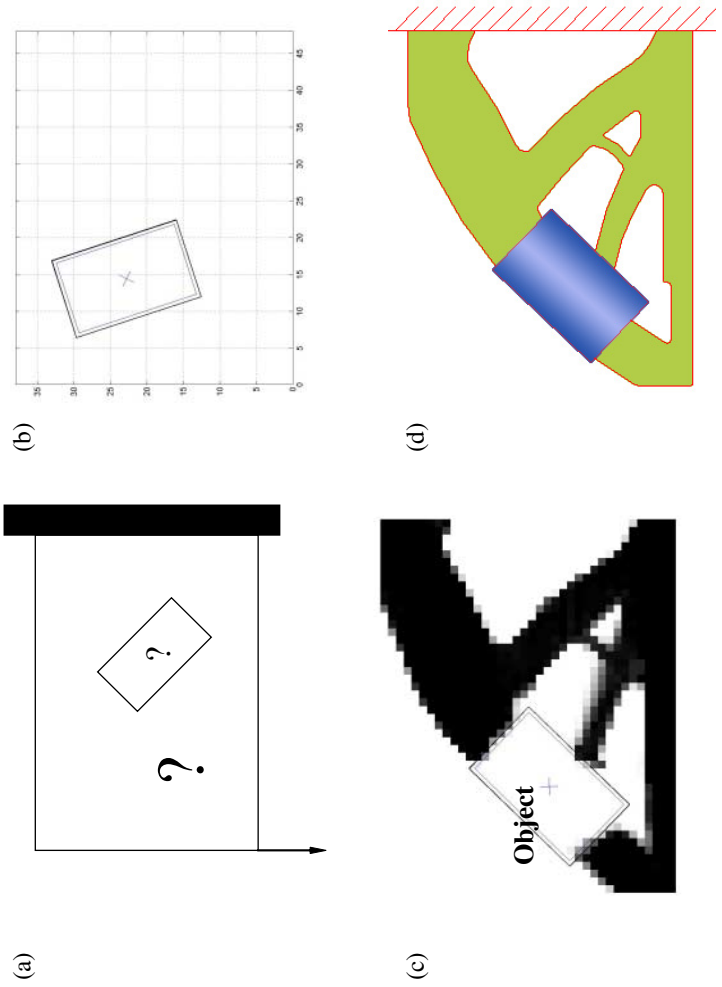

Figure 7. Example 1: (a) Problem specifications, (b) initial guess of the embedded rigid object, (c) optimal solution, and (d) interpretation of the solution. *(View this art in color at www.dekker.com.)*

Marcel Dekker, Inc.
270 Madison Avenue, New York, New York 10016

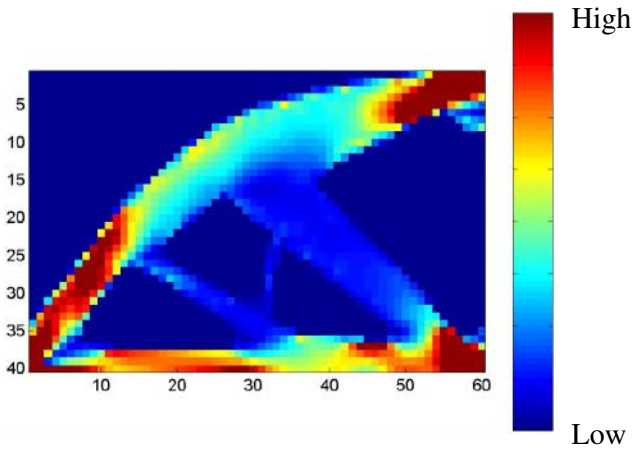

Figure 8. Von Mises stress distribution in the optimal structure for the case of no embedded objects. *(View this art in color at www.dekker.com.)*

at the two fixed supports. But there also two other places where the stress is large. So, what decides the location of the embedded object? Recall also from the beam example that the object is embedded where all of its length can be accommodated so that the stress is the same at its boundaries and is the largest. Hence, the algorithm chose the location shown in Fig. 7c. Notice further that unlike in the beam problem, the structure considered here is statically indeterminate and hence the stress distribution changes with the location of the object. Hence, the high-stress region of Fig. 8 does not exactly correspond to the location of embedded of the object but is too far from the high-stress region of sufficient length.

Two point forces and a moment are applied, as shown in Fig. 9a in the second example. The initial guess for the object position and orientation are shown in the figure. Optimal solution and the interpreted solution are shown in Figs. 9b and c, respectively. The optimal location of the embedded object can be explained in the same way as that of the previous example.

Embedding of Multiple Objects

Embedding multiple objects, as presented in the general formulation with m objects, poses no algorithmic difficulties other than increasing the

Marcel Dekker, Inc.
270 Madison Avenue, New York, New York 10016

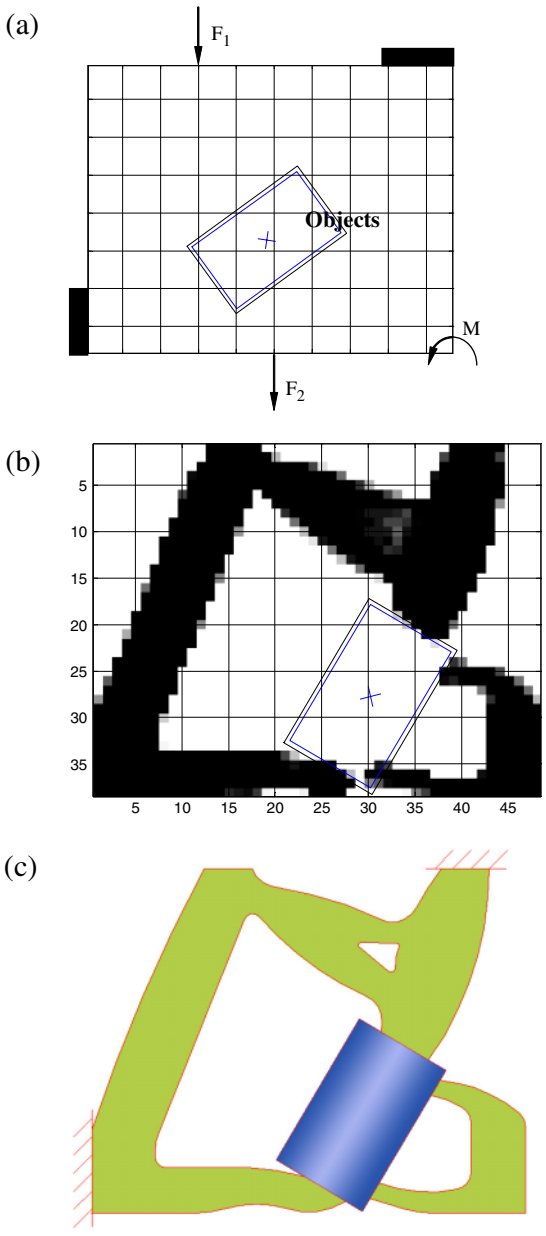

Figure 9. Example 2: (a) Problem specifications, (b) optimal solution, and (c) interpretation of the solution. *(View this art in color at www.dekker.com.)*

Marcel Dekker, Inc.
270 Madison Avenue, New York, New York 10016

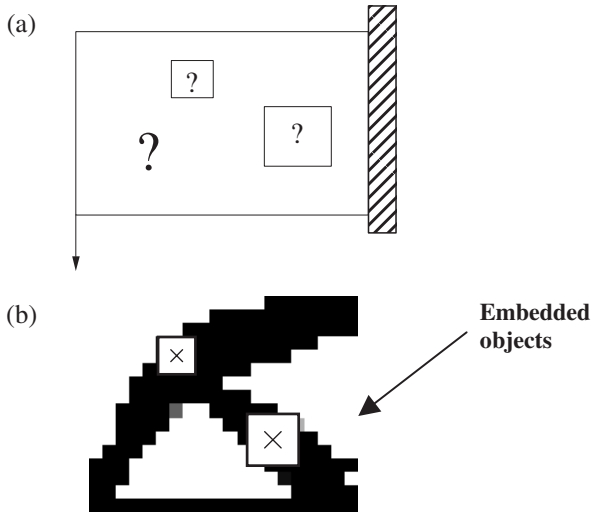

Figure 10. Example 3: (a) Design region and specifications and (b) optimal solution.

number of the variables. Two objects are included in the third example. Here, the rotation of the objects is not considered as might be necessary in some applications. The load is applied at the bottom-left end of the rectangular design region, and right edge is fixed. A 20×16 finite element model with 8 node quadrilateral elements was used. The problem specifications and the solution are shown in Figs. 10a and b.

Multicomponent System with Rigid Connections

The next two examples illustrate the special case of the general procedure. Here, we embed the rigid connections between the two components to create an assembled system of multiple components joined together with rigid connections such as the ones made with bolted or riveted fastening procedures. The design parameterization for this was presented earlier. In Example 4, the objective is to design the location of the two joints between two components, one of which is rigidly supported on one side, and the other being subjected to a load applied at the top-left corner. Rigid connections are permitted in a 8×25 grid design domain consisting of the overlapping portion of the two components. The specifications, optimal solution including the joint locations, and the interpreted solution are shown in Figs. 11a through c, respectively.

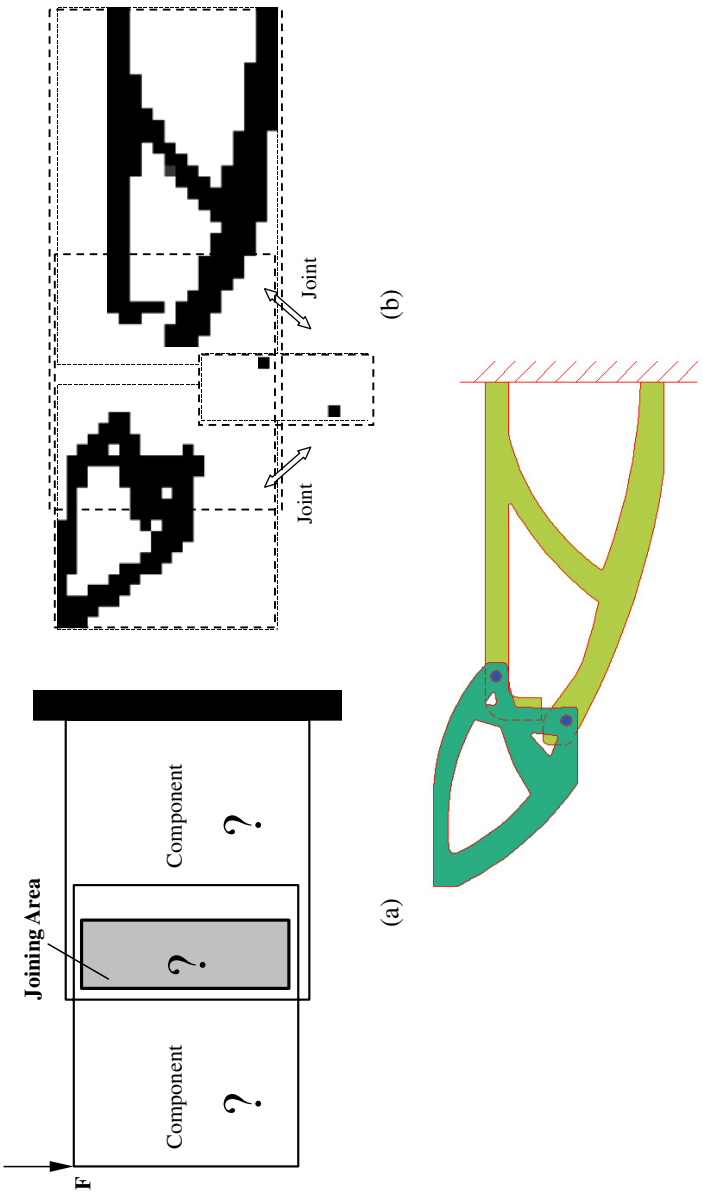

Figure 11. Example 4: A two-component system with two joint locations (a) problem specifications, (b) optimal solution, and (c) interpreted solution. *(View this art in color at www.dekker.com.)*

Marcel Dekker, Inc.
270 Madison Avenue, New York, New York 10016

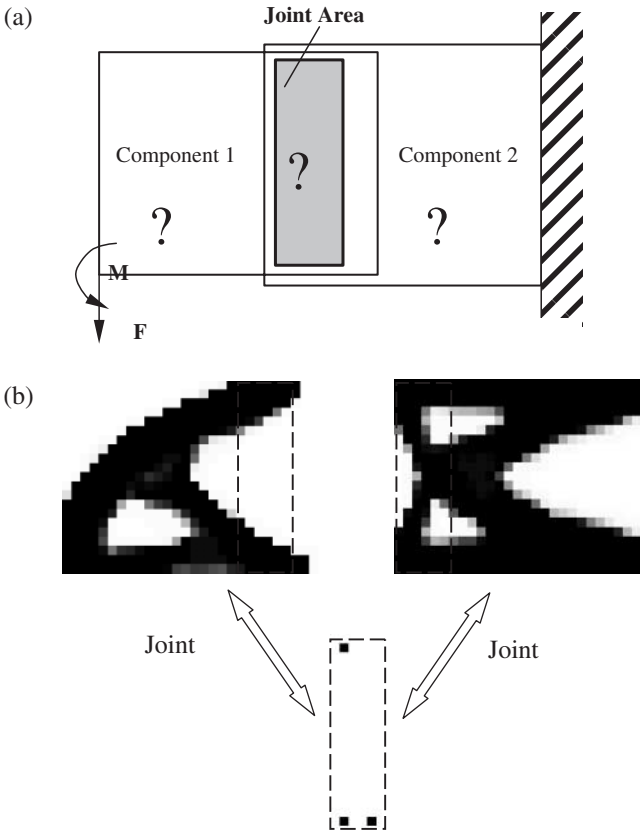

Figure 12. Example 5: A benchmark problem from (Chickermane and Gea, 1997). (a) Problem specification and (b) optimal solution.

Example 5 is the same as the previous example with the only difference that the loading is different, as shown in Fig. 12a. The optimal solution is shown in Fig. 12b. This example was taken from Chickermane and Gea (1997) and the solution we obtained is identical to the one reported there using a different solution technique.

Discussion and Future Work

From the viewpoint of optimal design of multiple component systems, the problem and formulation presented in this work are useful

in practice. As explained with a simple beam example and a few two-dimensional numerical examples, this problem is nonconvex. Hence, local optimization methods, such as the ones used in this section, can only give a local minimum, which may or may not be the best, i.e., the global minimum. Hence, it is desirable to develop either deterministic global optimization methods or find other means to find the global minimum. Since it may be computationally impractical, combining nondeterministic and deterministic algorithms may be explored. The nondeterministic methods, such as simulated annealing or genetic algorithms, may be able to provide a solution that is in the vicinity of the global minimum. That solution could be used as an initial guess for the deterministic algorithm. It will also be useful if further insight is gained into the problem for two-dimensional and three-dimensional cases of regular members, such as plates, shells, etc., or in the general case, by analysis along the lines of the analytical solution of the beam problem. This insight may help identify the global minimum without having to use a global optimization method. Another extension of this method is to embed active elements, such as piezoelectric, shape memory alloy and other elements, instead of only passive objects, as done in this work.

CONCLUSION

In this article, a new optimal embedding problem in topology optimization was presented. The objective of this problem is to position and orient given rigid objects in a given design region and also simultaneously design the topology of the connecting structure to have the overall assembly as stiff as possible. The topology optimization of multiple components with rigid or flexible connections among them becomes a special case of this problem. A new material interpolation scheme was presented to effect smooth variations in topology as well as the movement of embedded objects. Numerical examples show the feasibility of the method. This problem was observed to be nonconvex. The origin of nonconvexity was explained with a simple beam example that was solved analytically. Some future extensions of this problem were identified.

ACKNOWLEDGMENTS

The support from the National Science Foundation under grant #DMI 9800417 is gratefully acknowledged. The idea of embedding rigid

objects while designing the topology transpired in a discussion the second author had with Professor John Bassani, Mechanical Engineering and Applied Mechanics, University of Pennsylvania. Subsequent discussions with him are gratefully acknowledged.

REFERENCES

Bendsøe, M. P., Kikuchi, N. (1988). Generating optimal topologies in structural design using a homogenization method. *Computer Methods in Applied Mechanics and Engineering* 71:197–224.

Bendsøe, M. P., Sigmund, O. (2003). *Topology Optimization: Theory, Methods, and Applications*. New York: Springer.

Chickermane, H., Gea, H. C. (1997). Design of multi-component structural systems for optimal layout topology and joint locations. *Engineering with Computers* 13:235–243.

De Ruiter, M. J., Van Keulen, F. (2000). Topology optimization: approaching the material distribution problem using a topological function description. In: Topping, B. H. V., ed. *Computational Techniques for Materials, Composites, and Composite Structures*. Edinburgh, UK: Civil-Comp Press, 111–119.

Haftka, R. T., Gurdal, Z. (1989). *Elements of Structural Optimization*. Kluwer Academic Publishers.

Jiang, T., Chirehdast, M. (1997). A systems approach to structural topology optimization: designing optimal connections. *Journal of Mechanical Design* 119(1):40–47.

Johanson, R., Papalambros, P., Kikuchi, N. (1994). Simultaneous topology and material microstructure design. *Advances in Structural Optimization*, Proceedings, the Second World Conference on Computational Structures Technology Part 2 (of 4), Athens, Greece, August 30–September 1:143–149.

Kirsch, U. (1989). Optmal topologies of structures. *Applied Mechanics Reviews* 42(8):233–239.

Lyu, N., Saitou, K. (2003). *Decomposition-Based Assembly Synthesis of a 3D Body-In-White Model for Structural Stiffness*, Proceedings of the ASME 2003 International Mechanical Engineering Congress and RD&D Expo. Washington, D.C., USA, November 15–21.

Li, Y., Xin, X., Kikuchi, N., Saitou, K. (2001). *Optimal Shape and Location of Piezoelectric Materials for Topology Optimization of Flextensional Actuators*, Proc. of 2001 Genetic and Evolutionary Computations Conference, 1085–1089.

MARCEL DEKKER, INC.
270 Madison Avenue, New York, New York 10016

MATLAB. (2003). *Language for Technical Computing*. Waltham, MA: a software from MathWorks Inc.

Rozvany, G.I.N., Zhou, M., Gollub, M. (1989). Continuum type optimality criteria methods for large finite element systems with a displacement constraint, part 1. *Structural Optimization* 1:47–72.

Rozvany, G., Bendsøe, M., Kirsch, U. (1995). Layout optimization of structures. *Applied Mechanics Reviews* 48(2):41–119.

Wang, M., Wang, X., Guo, D. (2003). A level set method for structural topology optimization. *Computer Methods in Applied Mechanics and Engineering* 192:227–246.

Yetis, F. A., Saitou, K. (2002). Decomposition-based assembly synthesis based on structural considerations. *Journal of Mechanical Design* 124:593–601.

Yin, L., Ananthasuresh, G. K. (2001). Topology optimization of compliant mechanisms with multiple materials using a peak function material interpolation scheme. *Structural Multidisciplinary Optimization* 23(1):49–62.

Yin, L., Yang, W. (2001). Optimality criteria method for topology optimization under multiple constraints. *Computers and Structures* 79:1839–1850.

Received July 2003
Revised September 2003
Communicated by S. Azarm